

Magnetar Powered Ordinary Type IIP Supernovae

Tuguldur Sukhbold & Todd A. Thompson

Department of Astronomy and Center for Cosmology & Astro-Particle Physics, The Ohio State University, Columbus, Ohio 43210

25 April 2017

ABSTRACT

We investigate the properties of Type IIP supernovae that are dominantly powered by the rotational kinetic energy of the newly born neutron star. While the spin-down of a magnetar has previously been proposed as a viable energy source in the context of super-luminous supernovae, we show that a similar mechanism could produce both normal and peculiar Type IIP supernova light curves from red supergiant progenitors for a range of initial spin periods and equivalent dipole magnetic field strengths. Although the formation channel for such magnetars in a typical red supergiant progenitor is unknown, it is tantalizing that this proof of concept model is capable of producing ordinary Type IIP lightcurve properties, perhaps implying that rotation rate and magnetic field strength may play important roles in some ordinary looking Type IIP supernova explosions.

Key words: magnetars, supernovae

1 INTRODUCTION

The most common massive star supernovae in the universe, by number, are the explosions of red-supergiant (RSG) progenitors with initial masses of $\sim 9\text{--}18 M_{\odot}$ (Smartt 2015), and with kinetic energies on the order of $\sim 10^{51}$ ergs (Pejcha & Prieto 2015). These explosions create light curves of Type IIP, which gradually releases the shock deposited energy to produce roughly a constant luminosity for about 3 months (e.g., Filippenko 1997; Arcavi et al. 2012). The most intensely studied mechanism for these explosions is the delayed-neutrino driven mechanism (Colgate & White 1966; Arnett 1966; Bethe & Wilson 1985). While the neutrino mechanism is rather successful for the low energy explosions of lighter progenitors, there is no consensus yet in the supernova community on more massive progenitors that would provide the observed energies of typical supernovae (Janka et al. 2016, and references therein). Inspired by Bodenheimer & Ostriker (1974) and the application of neutron star models to luminous supernovae by Woosley (2010) and Kasen & Bildsten (2010), in this work we explore the scenario where the rotational energy source plays a dominant role throughout the explosion of a RSG progenitor.

Soon after the discovery of pulsars, it was suggested that an embedded pulsar might power the light curves and explosions of ordinary supernovae (Ostriker & Gunn 1971). More recently, the idea has gained new traction as a possible explanation for gamma-ray bursts (e.g., Usov 1992; Thompson et al. 2004; Uzdensky & MacFadyen 2006; Bucciantini et al. 2009; Metzger et al. 2011) and other unusual supernovae (Akiyama et al. 2003; Maeda et al. 2007). The pulsars required for these transients have atypical properties in that

their field strengths and rotation periods are extreme. Today, such models are thus commonly referred to as “magnetar” models rather than “pulsar” models.

Following Maeda et al. (2007), Woosley (2010) and Kasen & Bildsten (2010) independently promoted the idea that magnetars might underlie the production of a broad class of hydrogen poor super-luminous supernovae (SLSN-I), which are brighter than 10^{43} ergs s^{-1} for a time longer than typical Type Ia supernovae (a couple of weeks); see Quimby et al. (2011); Gal-Yam (2012) and Nicholl et al. (2015) for recent reviews of SLSN-I. Since 2010, many studies have interpreted the light curves of SLSN-I as the product of magnetar spin down (e.g., Benetti et al. 2014; Nicholl et al. 2013; Metzger et al. 2015; Dong et al. 2016).

Consider a scenario where a weak explosion is initiated in a RSG progenitor, and soon afterwards a magnetar, which formed from the collapse of a spinning progenitor core, starts to deposit energy. The exact nature of the formation is not well understood, an issue we revisit in § 3. In general, such a scenario would be representative of a case where the original neutrino wind becomes increasingly magnetically dominated as the proto-neutron star cools (Thompson et al. 2004; Metzger et al. 2007, 2011), eventually transitioning to a highly relativistic “pulsar”-type wind, depositing the pulsar rotational kinetic energy on the spin-down timescale.

Since the brightness and duration of the light curve plateau phase scales with the promptly deposited explosion energy as $\propto E^{5/6}$ and $\propto E^{-1/6}$ respectively (Popov 1993), the weak explosion alone, without any magnetar input, will create a long and dim transient compared to a typical Type IIP case. For the magnetar to transform this weak explosion into a typical one, it will need to inject a significant amount

arXiv:1704.06682v1 [astro-ph.HE] 21 Apr 2017

of energy in a short timescale, so that the plateau phase is brighter and transitions to the nebular phase sooner.

Approximating the initial rotational kinetic energy of the magnetar as $E_m \approx 2 \times 10^{52} P_{ms,i}^{-2}$ ergs, where $P_{ms,i}$ is the initial spin period in milliseconds, we can see that if it is to yield a final kinetic energy of an ordinary Type IIP explosion roughly between $0.5-2 \times 10^{51}$ ergs, the initial spin needs to be approximately between 3 and 6 ms. At late times (after the plateau phase) the tail of the light curve must be dominantly powered by the radioactivity, $L_m(t_{late}) < L_{Co}(t_{late})$, where L_m is the spin down luminosity and L_{Co} is the luminosity from the decay of ^{56}Co , resulting from a typical Type IIP yield of ^{56}Ni . For vacuum dipole spin-down the magnetar luminosity is $L_m \approx 10^{49} B_{15}^2 P_{ms}^{-4}$ ergs s^{-1} , where B_{15} is the magnetic field strength in 10^{15} G and an angle of $\pi/6$ was assumed between the rotational and magnetic axes. Taking t_{late} as 150 days and adopting a typical ^{56}Ni mass of $0.1 M_{\odot}$, we see that the spin down timescale, $t_m = E_m/L_m$, needs to be shorter than roughly a day for $3 < P_i < 6$ ms, or the constant dipole magnetic field needs to be larger than roughly 10^{15} G. At the other end, invoking more extreme conditions with $P_i \sim 1$ ms and field strengths of $> 10^{16}$ G may end up producing a typical IIP-like light curves in some situations, but will ultimately yield much higher energies and also may overproduce ^{56}Ni .

These basic considerations, though based on an idealized situation where the magnetar keeps indefinitely injecting energy, that is efficiently thermalized, based on vacuum dipole emission (braking index of $n = 3$) and a constant magnetic field strength, demonstrate that the rotational rates and magnetic field strengths of such IIP-powering magnetars must be larger than what is commonly inferred from pulsars. In this work, through a set of numerical experiments we explore the question of over what parameter space the classical magnetar spin down scenario can transform a weak explosion model of a RSG into one where the light curve characteristics, ^{56}Ni yields, and final kinetic energies are close to those of typical IIP supernovae.

2 NUMERICAL CALCULATIONS WITH KEPLER

We calculate a set of magnetar powered RSG explosion models using the 1D implicit hydrodynamic code KEPLER (Weaver et al. 1978). All calculations start with a RSG progenitor model from Sukhbold & Woosley (2014) with an initial mass of $15 M_{\odot}$. At the time of core collapse this model had a radius of $841 R_{\odot}$ and a total mass of $12.6 M_{\odot}$, of which the outermost $8.3 M_{\odot}$ was in the H-rich envelope. We first launch a weak explosion by using the moving inner boundary method, i.e. ‘‘piston-scheme’’ (Woosley & Weaver 1995; Sukhbold et al. 2016), so that the final kinetic energy of the ejecta is only about $\sim 5 \times 10^{49}$ ergs. This explosion synthesized roughly $0.16 M_{\odot}$ of ^{56}Ni , but due to late time fallback only about $\sim 0.015 M_{\odot}$ is ejected. The synthesized ^{56}Ni mass is on the large side because for this demonstration model the piston was deliberately placed at the edge of the iron core ($1.43 M_{\odot}$), which is significantly deeper than the mass cut that could represent a fully neutrino-driven explosion ($\sim 1.6 M_{\odot}$ for the same model in Sukhbold et al. (2016)). This choice primarily stems from our expectation that magnetar input, with our current description, would

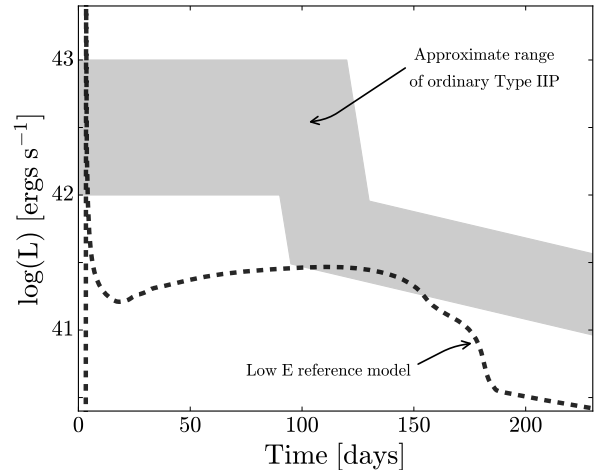


Figure 1. The light curve from the low energy 5×10^{49} ergs explosion (dashed black), without any further energy input, is shown in comparison with an approximate luminosity band of typical Type IIP supernovae. With much lower energy, the resulting light curve is much dimmer and has a long lasting plateau phase.

not significantly contribute to the ^{56}Ni synthesis, which we discuss further in § 3. As in Woosley (2010), we do not specify the physical nature of the explosion initiation.

As expected, this low energy explosion, without any additional energy input produces a long lasting dim transient (Fig. 1). Taking the scaling relations based on the survey of model Type IIP light curves from Sukhbold et al. (2016, Eqs. 15 and 17), one gets a plateau luminosity of $L_p = 2.3 \times 10^{41}$ ergs s^{-1} and a duration of the plateau, including the effects of radioactivity, is $\tau_p = 176$ days. These values are in a good agreement with the low energy explosion model shown in Fig. 1 as a dashed black curve. The plot also shows a rough luminosity range that represents the typical IIP light curves (light gray band): $10^{42} < L_p < 10^{43}$ ergs s^{-1} , $90 < \tau_p < 130$ days and the tail representing ^{56}Co decay luminosity for $0.05 < M_{Ni} < 0.2 M_{\odot}$ (Pejcha & Prieto 2015). Note that the ‘‘normal’’ light curve band corresponds to a much brighter and briefer plateaus than in the low energy explosion reference model (dashed curve in Fig. 1).

The piston that drives the low energy explosion first moves inward from its initial location at the edge of the iron core to a minimum radius of 10^7 cm in 0.25 seconds. Once it starts to move outwards, we begin to deposit energy to the inner part of the ejecta as heat according to the vacuum dipole spin-down formulation, $L_m(t) = E_m t_m^{-1} (1 + t/t_m)^{-2}$ ergs s^{-1} . The evolution of the ejecta is followed for ~ 350 days including the energy from radioactivity, and the light curves are approximately calculated with flux-limited diffusion. The magnetar parameters were varied from $B=10^{14-16}$ G for the constant dipole magnetic field strength at the equator, and between 1 and 10 ms for the initial rotational period. These spins correspond to a range of initial rotational kinetic energies between $0.2 - 20 \times 10^{51}$ ergs, and spin-down timescales between 20 seconds and 230 days.

Once the explosion is initiated, we expect a neutrino-driven wind to emerge from the cooling proto-neutron star

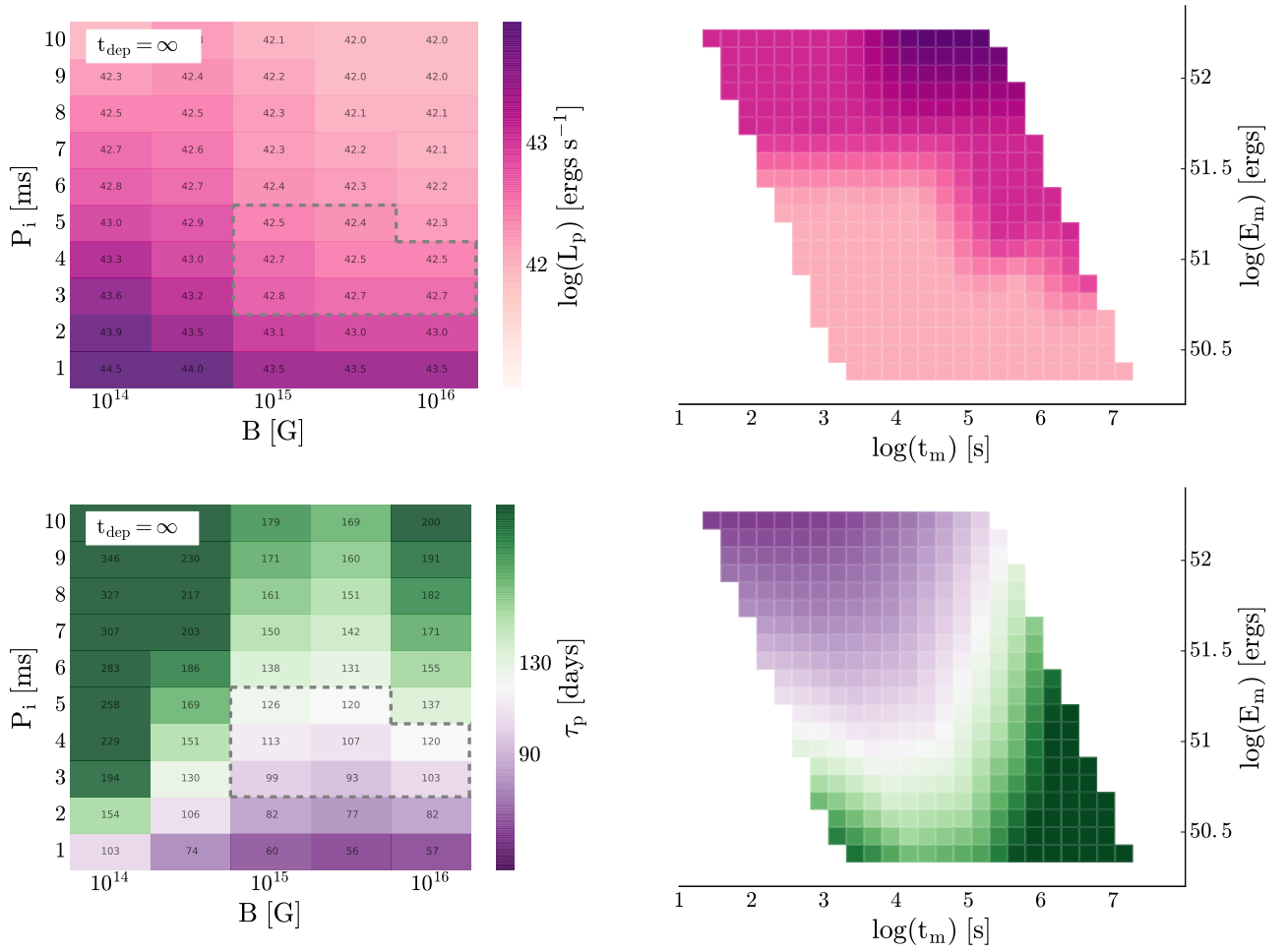


Figure 2. Heatmaps of lightcurve plateau luminosity (top) and durations (bottom) for magnetar powered light curves as a function of the magnetic field strength B and the initial spin P_i (left), and as a function of initial spin-down timescale t_m and rotational kinetic energy E_m (right, interpolated). Each case starts with low energy (5×10^{49} ergs) piston explosion of a $M_{ZAMS}=15 M_{\odot}$ RSG progenitor, and the magnetar energy was deposited from 0.25 seconds until the end of calculation. The plateau duration, τ_p , is measured as the time from the explosion until when the photospheric radius dips below 10^{14} cm, and the plateau luminosity is measured as $L_p = L(\tau_p/2)$, see text for details. Regions surrounded by dashed lines in each panel denote the ranges of initial magnetar spin and magnetic field strength that produces typical Type IIP light curves with $90 < \tau_p < 130$ days and $42 < \log(L_p) < 43$ ergs s^{-1} .

(Duncan et al. 1986; Janka & Mueller 1996; Burrows et al. 1995). For a given magnetic field strength and spin period, the flow will become increasingly relativistic over the Kelvin-Helmholz cooling timescale as the Alfvén point in the flow approaches the light cylinder (Thompson et al. 2004; Metzger et al. 2007, 2011). The energy injection rate at these very early times is higher than implied by the vacuum dipole expression for the same B and P , and may be complicated as the neutron star contracts and its convection changes character throughout the cooling epoch (Pons et al. 1999; Roberts et al. 2012). However, because the long-term spin-down behavior more directly affects the eventual lightcurve shape and dynamics than the detailed evolution at these very early times, we simply assume the vacuum dipole energy injection formula. For these purposes B and P should be interpreted as defining the rotation energy reservoir and the reference energy loss rate.

The effect of late time magnetar powered light curves have been extensively studied in the context of SLSN-I

emerging from stripped cores (e.g., Inserra et al. 2013). In general, with shorter spin down timescale, most of the magnetar energy input is lost to adiabatic expansion, while with longer timescale more energy is channeled into radiation and produces luminous light curves. The same generic behavior is also seen in our calculations, however, with the extended envelope of the RSG progenitor the light curves present a diverse structure, and with a larger ejecta mass the magnetar powered Type II light curves are generally less luminous than Type I cases.

Figure 2 shows the resulting light curve plateau properties from magnetar powered explosions when the energy was injected until the end of calculation (~ 350 days). The plateau duration, τ_p , was conservatively measured as the time span from the beginning of explosion until when the photospheric radius dips below 10^{14} cm, while the plateau luminosity was measured in the middle of the plateau as $L_p = L(\tau_p/2)$. These conditions apply well to all calculations, except those with the weakest field strengths and slow-

est initial spins. In those models, the spin-down timescale is comparable to the calculation time and in a few cases the photospheric radius does not reach its maximum within 300 days, resulting in very long τ_D .

For a given initial spin, the most luminous light curves emerge from models with weakest field strengths since the spin-down timescale is longest. For a given field strength, the spin-down timescale decreases with faster initial spin, but due to the increasing energy budget, much more energy is channeled into radiation compared to a slower spin model. The most luminous model with 10^{14} G and initial spin of $P_{\text{ms}}=1$ exceeds a peak luminosity of a few times 10^{44} ergs s^{-1} . In models with stronger fields the plateau luminosity never exceeds of 10^{43} ergs s^{-1} , except the few with the fastest initial spins. From the other side, the least luminous models come from strongest fields and lowest energy budgets. In all of these calculations, the deposited energy is much larger than the initial weak explosion energy of 5×10^{49} ergs, and thus all the models are significantly more luminous than the reference light curve shown in Fig. 1.

The behaviour of the plateau duration is slightly more complicated. With more energy deposited promptly (i.e. shorter spin-down timescale), the ejecta will be strongly ionized and will expand faster, resulting in brighter and briefer plateaus. While with more gradual deposition, the magnetar energy extends the plateau phase by supporting ionization, in much the same way as done in through radioactive decay energy (see Kasen & Woosley 2009). This is why the plateau duration increases with slower initial spin, for a given field strength. However, note that for a given initial spin the plateau duration first shortens with increasing field strength, and then starts to lengthen again for $B > 10^{15}$ G. For smaller field strengths, the spin-down luminosity is always greater than or comparable to the luminosity from radioactive decay, while at higher field strengths it is always much weaker than the decay luminosity at late times.

Consistent with the results found in Suwa & Tominaga (2015), none of our models produced extra ^{56}Ni in addition to the initial explosion. However, in all of the models the fallback that occurs in the original reference model does not occur and thus they all receive power from the decay of $0.16 M_{\odot}$ ^{56}Ni . This has little relevance for the plateau phase of the lightcurve when the magnetar is slowly depositing energy, but it can significantly extend the plateau phase when nearly all of magnetar energy is deposited promptly. If the energy contribution from radioactivity is removed, the plateau duration monotonically decreases with increasing field strength as expected.

The regions bounded by a dashed line in Fig. 2 highlight the models that have similar plateau durations and luminosities to typical Type IIP supernovae. Note the plateau luminosities are between 10^{42} and 10^{43} ergs s^{-1} for most models with $P_1 > 3$ ms, and so this region is primarily bounded by the plateau durations, except when the spin-down timescale is long with weaker field strengths and slower initial spins. As expected (§ 1), this region covers mostly models that were powered by magnetars with P_1 roughly between 3 and 6 ms, and B stronger than 10^{15} G. For stronger field strengths there is a slight preference for a slower initial spin, since the radioactive extension of the plateau becomes less relevant with increasing rotational energy of the magnetar.

Figure 3 shows light curves (colored curves) from the

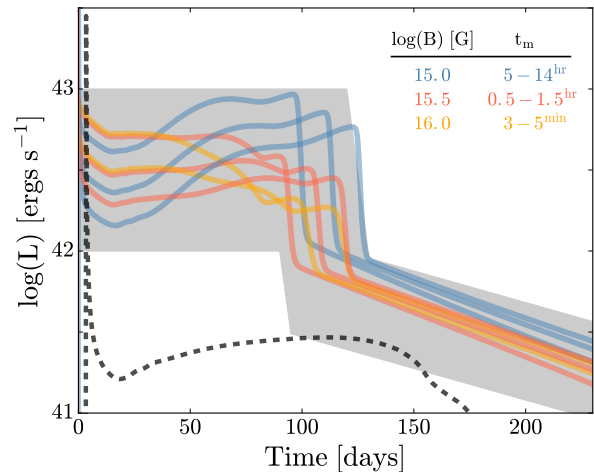


Figure 3. Magnetar powered light curves (colored curves) from the highlighted region in Fig. 2, where the models have plateau luminosities and durations that lie within the range of observed ordinary Type IIP supernovae (gray band from Fig. 1). The light curves from magnetars with $\log(B)=15$ G are shown in blue, $\log(B)=15.5$ G shown in red, and with $\log(B)=16$ G are shown in orange. For a given field strength (curves from a given color), with increasing initial rotational energy (smaller P_1) the light curve plateau phase is brighter and shorter. For a given initial spin, with longer the spin-down timescale (smaller B) the plateau phase brightens in time due to persistent magnetar luminosity at late times, while with shorter spin-down timescale the plateau is roughly constant or dimming with time. Observed Type IIP light curves with rising plateaus are often associated with blue supergiant progenitors, but here we show that late time magnetar energy deposition can result in such light curves from a normal RSG progenitor.

models that lie in the region bounded by dashed lines in Fig. 2. As in Fig. 1, it also shows the reference weak explosion model without any magnetar input (dashed curve), and the approximate luminosity band (gray band) for “typical” Type IIP light curves. Note that while some light curves have a fairly constant luminosity during the plateau phase (red), others are sharply increasing (blue) or decreasing (orange) until before they transition to nebular phase. The increasing luminosity during the plateau phase results when the magnetar deposition dominates for a time comparable or longer than the effective diffusion timescale of the ejecta, so that without much prompt energy deposition it is dimmer in the first few weeks and it gradually brightens due to the magnetar luminosity at later times. Also note that the tail is slightly brighter than models with shorter spin-down due to magnetar input, even though all of the models receive the same amount of radioactive energy. In general, this effect is even more prominent for weaker field strengths than 10^{15} G, where the plateau keeps rising for hundreds of days and several orders of magnitude in luminosity, but the resulting light curves are well beyond what we consider as typical of Type IIP. With shorter spin-down times, the magnetar efficiently deposits energy promptly and therefore the early light curve appears brighter, but it stays roughly constant or keeps dimming afterwards as the ejecta expands much faster without experiencing much magnetar energy input at later times.

These model light curves are consistent with the diversity seen in the observations (e.g., [Arcavi et al. 2012](#)). The most notable are those with increasing plateau luminosity, which are often classified as peculiar and associated with a blue supergiant progenitor (e.g., [Taddia et al. 2016](#)) due to their similarity with SN1987A. With the explosion of a compact progenitor, the light curve is initially less luminous due to the energy lost in adiabatic expansion. However, our calculations demonstrate that such light curves can emerge from RSG progenitors when their explosions are powered by magnetars. In this case, however, the progenitor is already extended to begin with, and the light curve starts from a lower luminosity because of weaker recombination of the envelope and gradually brightens when the magnetar keeps depositing significant amount of energy at late times.

3 DISCUSSION

We have explored the light curves emerging from an explosion of a RSG progenitor that was initiated by a weak piston and followed by energy deposition from a magnetar. Through a set of spherically symmetric hydrodynamical calculations with approximate radiation transport, we have shown that for a narrow range of magnetar parameters, the resulting light curves resemble what we observe in ordinary Type IIP supernova explosions. For the progenitor explored, when the initial spin of the magnetar is between 3 and 5 ms, and its dipole magnetic field is strength greater than 10^{15} G, the energy deposition through vacuum dipole spin-down transforms the long-lasting dim transient, produced by the weak piston-driven explosion alone, into transients with plateau luminosities of 10^{42-43} ergs s^{-1} and durations of 90-130 days. The final kinetic energies of the ejecta are in the expected range ($\sim 0.8-2 \times 10^{51}$ ergs) and since the magnetar deposition does not produce any extra ^{56}Ni , the magnetar energy input with a short spin-down time results in radioactively powered light curve tails seen in ordinary Type IIP supernovae, as long as enough is synthesized through the initial weak explosion

The above-mentioned preferred range for the magnetar spin period and magnetic field strength correspond in part to the some of the employed assumptions. For example, if the initial prompt energy assumed is higher, then lower initial spin rates would yield typical Type IIP energies at late times. When we repeat the calculation using a RSG progenitor with an initial mass of $12 M_{\odot}$, and with a prompt explosion energy of 8×10^{49} ergs, the corresponding range of P_i that produces typical Type IIP light curves shifts to $\sim 4-7$ ms, because the prompt non-magnetar component of the energy budget for the explosion is larger than in the $15 M_{\odot}$ progenitor shown in Fig. 1. But as long as this prompt explosion energy is much smaller than the rotational kinetic energy of the magnetar, the same generic results will hold - initial period of a few ms ($P_i \sim (20/(1 - E_{\text{prompt}}/10^{51}))^{1/2}$ ms) and a strong field strength of $B > 10^{15}$ G for a relatively fast initial spin-down time. The dependence on the progenitor structure is rather small since for solar metallicity the ejecta masses and the envelope masses are fairly similar for progenitors with initial masses between $10 - 25 M_{\odot}$ (e.g., [Sukhbold & Woosley 2014](#)), which are responsible for majority of Type IIP supernovae ([Smartt 2015](#)),

Another possibility is that many of the neutron stars born in Type IIP supernovae start with high, but short-lived, magnetic fields generated by a dynamo mechanism as the neutron star cools and convects (e.g., [Duncan & Thompson 1992](#)). To probe this scenario, we have re-calculated all of the models but depositing energy only during the initial 50 seconds (Fig. 4). The amount of energy deposited during the initial time t is approximately $\Delta E = E_{m,it}(t + t_m)^{-1}$. When the spin-down timescale is much larger the deposition time it approaches $L_m t$. Therefore for $B < 10^{15}$ G and $P_i > 4$ ms the energy deposition for only 50 seconds does not result in any noticeable effect on the light curve. Accordingly the range of B and P_i that results in ordinary Type IIP plateau characteristics shifts to ~ 1 ms and $\sim 10^{16}$ G range. In general, the magnetar spin-down luminosity during the initial 50 seconds is highly uncertain, since the neutron star is convective and its wind rapidly evolves ([Thompson et al. 2004](#); [Metzger et al. 2011](#)). Therefore the magnetic field strengths in Fig. 4 should be thought of as a proxy for the time-averaged magnetar luminosity during the initial 50 seconds. Future models should explore how pulsar driven shells might synthesize of ^{56}Ni and power the shockwave, as it moves through dense inner core of the ejecta.

Although the evidence is growing to connect the nature of the most energetic explosions (e.g., long duration gamma-ray bursts and SLSN-I) to a rotational energy source, imagining a magnetar being responsible for some ordinary Type IIP explosions is not too far fetched. So far we have detected only a few dozen magnetars in the Galaxy, and some of them are known to reside in Type II supernova remnants (based on their large ejecta mass) that seem to indicate a canonical explosion energy of $\sim 10^{51}$ ergs ([Vink & Kuiper 2006](#)). One can also roughly approximate the vacuum spin-down periods for the 5 magnetars listed in the the McGill Online Magnetar Catalogue¹ ([Olausen & Kaspi 2014](#)), that have a clear association with a supernova remnant. Using the measured surface dipole field strengths, assuming a braking index of $n = 3$, and $P_i = 4$ ms, would bring the vacuum spin-down periods at the estimated ages (as $P_i(1 + t_{\text{age}}/t_m)^{1/2}$) to of order the measured periods. This of course ignores known factors of the evolving magnetic field strength, both potentially on short time scales due to cooling, convection, and dynamo effects, and on long time scales due to non-MHD dissipation as in [Viganò et al. \(2013\)](#); [Gullón et al. \(2015\)](#). Nevertheless this is suggestive that magnetars might be somehow connected to some ordinary Type IIP supernovae.

Given the presupernova conditions for a typical solar metallicity RSG progenitor from stellar evolution calculations with dynamo processes, it is not straightforward to obtain proto-neutron star magnetic fields greater than 10^{15} G and initial spins of just few ms ([Heger et al. 2005](#)). Magnetic torques during the evolution result in a slower spinning iron core, and without invoking magneto-rotational instabilities, or some other magnetic amplification processes, the flux compression alone is not sufficient for a strong enough field. However, we note that the general problem of understanding the effective angular momentum transport in stellar interiors is still very much an open question. Until the existing theories are tested against asteroseismological mea-

¹ <http://www.physics.mcgill.ca/~pulsar/magnetar/main.html>

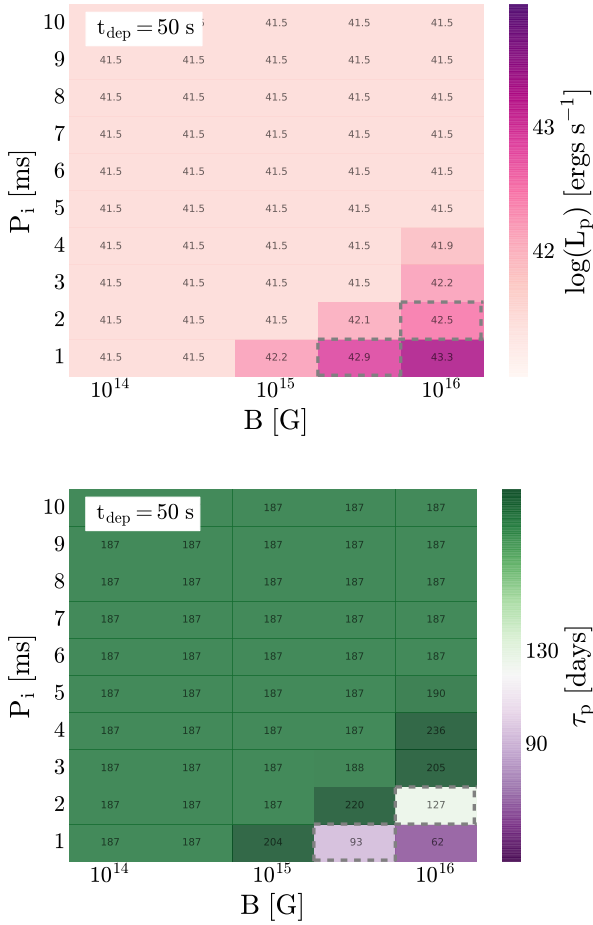


Figure 4. Same as Fig. 2, but here the magnetar deposits energy only during the initial 50 seconds. The range of magnetar parameters that transforms the weak explosion into a typical Type IIP light curve is now $\log(B) > 10^{15}$ G and $P_i < 3$ ms.

surements, which are the only way of probing the internal rotation profiles of evolved stars. The existing seismological data, though only available for much lower mass stars at the moment, already challenge our current understanding of angular momentum transport in redgiants (e.g., [Deheuvels et al. 2015](#); [Tayar & Pinsonneault 2013](#)).

In some ways it is not surprising that magnetar models can fit nearly all kinds of explosion light curves, including some regular Type IIP, when a big fraction of the explosion energy reservoir is replaced with a simple model that allows us to conveniently control its budget (initial spin) and injection rate (constant dipole magnetic field strength). This of course could be a fine-tuning, or interesting evidence that the supernova mechanism is connected to rotation and magnetic fields.

ACKNOWLEDGMENTS

We thank Stan Woosley, Chris Kochanek, Laura Lopez, Katie Auchetl, Ondrej Pejcha and John Beacom for helpful discussions and comments. We also thank Alex Heger

for his contributions in developing the KEPLER code. TS is partly supported by NSF (PHY-1404311) to John Beacom.

REFERENCES

- Akiyama, S., Wheeler, J. C., Meier, D. L., & Lichtenstadt, I. 2003, *ApJ*, 584, 954
- Arcavi, I., Gal-Yam, A., Cenko, S. B., et al. 2012, *ApJ*, 756, L30
- Arnett, W. D. 1966, *Canadian Journal of Physics*, 44, 2553
- Benetti, S., Nicholl, M., Cappellaro, E., et al. 2014, *MNRAS*, 441, 289
- Bethe, H. A., & Wilson, J. R. 1985, *ApJ*, 295, 14
- Bodenheimer, P., & Ostriker, J. P. 1974, *ApJ*, 191, 465
- Bucciantini, N., Quataert, E., Metzger, B. D., et al. 2009, *MNRAS*, 396, 2038
- Burrows, A., Hayes, J., & Fryxell, B. A. 1995, *ApJ*, 450, 830
- Colgate, S. A., & White, R. H. 1966, *ApJ*, 143, 626
- Deheuvels, S., Ballot, J., Beck, P. G., et al. 2015, *A&A*, 580, A96
- Dong, S., Shappee, B. J., Prieto, J. L., et al. 2016, *Science*, 351, 257
- Duncan, R. C., Shapiro, S. L., & Wasserman, I. 1986, *ApJ*, 309, 141
- Duncan, R. C., & Thompson, C. 1992, *ApJ*, 392, L9
- Filippenko, A. V. 1997, *ARA&A*, 35, 309
- Gal-Yam, A. 2012, *Science*, 337, 927
- Gullón, M., Pons, J. A., Miralles, J. A., et al. 2015, *MNRAS*, 454, 615
- Heger, A., Woosley, S. E., & Spruit, H. C. 2005, *ApJ*, 626, 350
- Inserra, C., Smartt, S. J., Jerkstrand, A., et al. 2013, *ApJ*, 770, 128
- Janka, H.-T., & Mueller, E. 1996, *A&A*, 306, 167
- Janka, H.-T., Melson, T., & Summa, A. 2016, arXiv:1602.05576
- Kasen, D., & Woosley, S. E. 2009, *ApJ*, 703, 2205
- Kasen, D., & Bildsten, L. 2010, *ApJ*, 717, 245
- Maeda, K., Tanaka, M., Nomoto, K., et al. 2007, *ApJ*, 666, 1069
- Metzger, B. D., Thompson, T. A., & Quataert, E. 2007, *ApJ*, 659, 561
- Metzger, B. D., Giannios, D., Thompson, T. A., Bucciantini, N., & Quataert, E. 2011, *MNRAS*, 413, 2031
- Metzger, B. D., Margalit, B., Kasen, D., & Quataert, E. 2015, *MNRAS*, 454, 3311
- Nicholl, M., Smartt, S. J., Jerkstrand, A., et al. 2013, *Nature*, 502, 346
- Nicholl, M., Smartt, S. J., Jerkstrand, A., et al. 2015, *MNRAS*, 452, 3869
- Olausen, S. A., & Kaspi, V. M. 2014, *ApJS*, 212, 6
- Ostriker, J. P., & Gunn, J. E. 1971, *ApJ*, 164, L95
- Pejcha, O., & Prieto, J. L. 2015, *ApJ*, 806, 225
- Pons, J. A., Reddy, S., Prakash, M., Lattimer, J. M., & Miralles, J. A. 1999, *ApJ*, 513, 780
- Popov, D. V. 1993, *ApJ*, 414, 712
- Quimby, R. M., Kulkarni, S. R., Kasliwal, M. M., et al. 2011, *Nature*, 474, 487
- Roberts, L. F., Shen, G., Cirigliano, V., et al. 2012, *Physical Review Letters*, 108, 061103
- Smartt, S. J. 2015, *PASA*, 32, e016
- Sukhbold, T., & Woosley, S. E. 2014, *ApJ*, 783, 10
- Sukhbold, T., Ertl, T., Woosley, S. E., Brown, J. M., & Janka, H.-T. 2016, *ApJ*, 821, 38
- Suwa, Y., & Tominaga, N. 2015, *MNRAS*, 451, 282
- Taddia, F., Sollerman, J., Fremling, C., et al. 2016, *A&A*, 588, A5
- Tayar, J., & Pinsonneault, M. H. 2013, *ApJ*, 775, L1
- Thompson, T. A., Chang, P., & Quataert, E. 2004, *ApJ*, 611, 380
- Usov, V. V. 1992, *Nature*, 357, 472
- Uzdensky, D. A., & MacFadyen, A. I. 2006, *ApJ*, 647, 1192
- Viganò, D., Rea, N., Pons, J. A., et al. 2013, *MNRAS*, 434, 123

- Vink, J., & Kuiper, L. 2006, MNRAS, 370, L14
Weaver, T. A., Zimmerman, G. B., & Woosley, S. E. 1978, ApJ,
225,1021
Woosley, S. E. 2010, ApJ, 719, L204
Woosley, S. E., & Weaver, T. A. 1995, ApJS, 101, 181